Evaluation and illustration of the properties of Metamaterials using field summation

Olivier Acher[1], Jean-Marie Lerat[2] and Nicolas Malléjac[1]

[1]*CEA Le Ripault, BP 16,F- 37260 Monts,France*
[2]*SATIMO, 22 avenue de la Baltique, 91953 Courtaboeuf, France*
olivier.acher@cea.fr

Abstract: The prediction and the engineering of the electromagnetic properties of metamaterials are increasingly important issues. Recently, several approaches have been proposed to compute these properties through appropriate averages of local fields within the unit cell. In particular, we proposed a Field Summation method that has been used successfully to determine either analytically or numerically the effective properties of different composites and metamaterials. But this method also provides interesting clues for understanding the behaviour of these materials. It helps chose appropriate planes to visualize the fields using electromagnetic simulation software, and understand behaviours leading to either positive or negative effective parameters, with either small or large values. It helps establish whether the materials can be adequately described by effective parameters.

OCIS codes: (160.4760) Optical properties; (350.4010) Microwaves

References and links

1. K. Aydin, K. Guven, M. Kafesaki, L. Zhang, C. M. Soukoulis, and E. Ozbay, "Experimental observation of true left-handed transmission peak in metamaterials," Opt. Lett. **29**, 2623 (2004).
2. C. Enkrich, M. Wegener, S. Linden, S. Burger, L. Zschiedrich, F. Schmidt, J. F. Zhou, Th. Koschny, and C. M. Soukoulis, "Magnetic metamaterials at telecommunication and visible frequencies," Phys. Rev. Lett. **95**, 203901 (2005).
3. T. Decoopman, A. Marteau, E. Lheurette, O. Vanbésien and D. Lippens, "Left-Handed Electromagnetic Properties of Split-Ring Resonator and Wire Loaded Transmission Line in a Fin-Line Technology," IEEE Trans. MTT **54**, 1451-1457 (2006).
4. V. M. Shalaev, W. Cai, U. K. Chettiar, H.-K. Yuan, A. K. Sarychev, V. P. Drachev, and A. V. Kildishev, "Negative index of refraction in optical metamaterials," Opt. Lett. **30**, 3356-3358 (2005).
5. A. N. Grigorenko, A. K. Geim, H. F. Gleeson, Y. Zhang, A. A. Firsov, I. Y. Khrushchev, and J. Petrovic, "Nanofabricated media with negative permeability at visible frequencies," Nature **438**, 335-338 (2005).
6. J. B. Pendry, A. J. Holden, D. J. Robbins, and W. J. Stewart, "Magnetism from conductors and enhanced nonlinear phenomena," IEEE Trans. Microwave Theory Tech. **47**, 2075-2084 (1999).
7. D. R. Smith, W. J. Padilla, D. C. Vier, S. C. Nemat-Nasser, and S. Schultz, "Composite medium with simultaneously negative permeability and permittivity," Phys. Rev. Lett. **84**, 4184 (2000).
8. V. Lomakin, Y. Fainman, Y. Urzhumov, and G. Shvets, "Doubly negative metamaterials in the near infrared and visible regimes based on thin film nanocomposites," Opt. Express **14**, 11164-11177 (2006).
9. W. J. Padilla, D. R. Smith, and D. N. Basov, "Spectroscopy of metamaterials from infrared to optical frequencies," J. Opt. Soc. Am. B **23**, 404 (2006).
10. O. Reynet, O. Acher, "Voltage controlled metamaterial," Appl. Phys. Lett. **84**, 1198-2000 (2004).
11. S. Tretyakov, *Analytical modelling in Applied Electromagnetics*, (Artech House, 2003).
12. K. N. Rozanov and E. A. Preobrazhenskii, "Synthesis of wideband radar absorbers based on complex media composed from active electric Dipoles," J. Commun. Technol. Electron. **50**, 858-864 (2005).
13. A.-L. Adenot-Engelvin, C. Dudek and O. Acher, "Microwave permeability of metamaterials based on ferromagnetic composites," J. Magn. Magn. Mater. **300**, 33-37 (2006).
14. A. Alù, A. Salandrino, and N. Engheta, "Negative effective permeability and left-handed materials at optical frequencies," Opt. Express **14**, 1557-1567 (2006).
15. R. Ziolkowski, "Pulsed and CW Gaussian beam interactions with double negative metamaterial slabs," Opt. Express **11**, 662-681 (2003).
16. D. Seetharamdoo, R. Sauleau, K. Mahdjoubi and A.-C. Tarot, "Effective parameters of resonant negative refractive index metamaterials: Interpretation and validity," J. Appl. Phys. **98**, 063505 (2005).

#77425 - $15.00 USD Received 27 November 2006; revised 19 January 2007; accepted 19 January 2007

17. B. I. Popa and S. A. Cummer, "Wave fields measured inside a negative refractive index metamaterial," Appl. Phys. Lett. **85**, 4564-4566 (2004).
18. D. R. Smith and J. B. Pendry, "Homogenization of metamaterials by field averaging," J. Opt. Soc. Am. B **23**, 391-403 (2006).
19. J.-M. Lerat, N. Malléjac and O. Acher, "Determination of the effective parameters of a metamaterial by field summation method," J. Appl. Phys. **100**, 084908 (2006).
20. T. Driscoll, D. N. Basov, A. F. Starr, P. M. Rye, S. Nemat-Nasser, D. Schurig and D. R. Smith, "Free-space microwave focusing by a negative-index gradient lens," Appl. Phys. Lett. **88**, 081101 (2006).
21. A. Cho, "Voilà ! Cloak of Invisibility Unveiled," Science **314**, 403 (2006).
22. D. R. Smith, S. Schultz, P. Markos and C. M. Soukoulis, "Determination of effective permittivity and permeability of metamaterials from reflection and transmission coefficients," Phys. Rev. B **65**, 195104 (2002).
23. O. Acher, A. –L. Adenot, and F. Duverger, "Fresnel coefficients at an interface with a lamellar composite material," Phys. Rev. B **62**, 13748 (2000).
24. S. M. Rytov, "Electromagnetic properties of a finely stratified medium," Sov. Phys. JETP **2**, 466-475 (1956).
25. A. N. Lagarkov, A. K. Sarychev, Y. R. Smychkovich and A. P. Vinogradov, "Effective Medium Theory for microwave dielectric constant and magnetic permeability of conducting stick composites," J. Electromagn. Waves Appl. **6**, 1159 (1992).
26. O. Acher, A. –L. Adenot, F. Lubrano, F. Duverger, "Low density artificial magnetic composites," J. Appl. Phys., **85**, 4639-4641 (1999).
27. O. Reynet, A. –L. Adenot, S. Deprot, O. Acher, M. Latrach, "Effect of the magnetic properties of inclusions on the high-frequency dielectric response of diluted composites," Phys. Rev. B **66**, 94412 (2002).
28. M. V. Gorkunov, S. A. Gredeskul, I. V. Shadrinov and Y. S. Kivshar, "Effect of microscopic disorder on magnetic properties of metamaterials," Phys. Rev. E **73**, 056605 (2006).
29. O. Acher, M. Ledieu, A.–L. Adenot and O. Reynet, "Microwave properties of diluted composites made of magnetic wires with giant magneto-impedance effect," IEEE Trans. Magn., **39**, 3085-3090 (2003).
30. D. Maystre and S. Enoch, "Perfect lenses made with left-handed materilas: Alice's mirror ?," J. Opt. Soc. Am. A **21**, 122-131 (2004).
31. T. Decoopman, G. Tayeb, S. Enoch, D. Maystre and B Gralak, "Photonic Crystla Lens: From Negative Refraction and Negative Index to Negative Permittivity and Permeability," Phys. Rev. Lett. **97**, 073905 (2006).

1. Introduction

Metamaterials have raised a significant interest in a wide community ranging from microwave to optics [1, 2, 3, 4, 5] within a few years after the seminal work of Pendry [6] and Smith [7]. Obtaining negative values for the permeability μ is a fundamental requirement in obtaining negative index metamaterials, but also a very new and intriguing feature when this is achieved in the optical region [8, 9]. It has been shown that negative permeabilities can be obtained through a variety of approaches, either inductive patterns such as split rings [7], loops connected to electronics [10, 11, 12], inductive pattern loaded with a magnetic core [13], pairs of conducting elements [2], and many others [8, 14]. It is of fundamental importance to be able to compute the values of μ, but also to have intuitive representations of what makes it negative in a given frequency range. Simulation software has already been used extensively to investigate and illustrate waves impinging on a negative index material [8, 14, 15, 16]. More recently, direct measurements of the electromagnetic fields inside metamaterials has been demonstrated, and provide both direct evidence and inspiring understanding of negative index metamaterials [17]. But to our knowledge, plotting the electromagnetic field within the unit cell of a metamaterial has not yet been exploited to provide visual and inspiring insights on the sign and magnitude of the permeability and permittivity. In addition, it is desirable that the effective parameters can be computed from the fields determined in a unit cell of a metamaterial. In 2006, two approaches termed "field averaging" [18] or "field summation" [19] methods have been applied to metamaterials in order to compute their values of ε and μ from proper field averages within the unit cell. These approaches are particularly valuable for the study of metamaterials with gradient properties, that attract a strong attention either for lenses [20] or for "invisibility cloaks" [21]. Such gradient metamaterials can be modelled through electromagnetic simulation software, but so-called retrieval procedures [22] are not adequate to extract the local (and possibly anisotropic) effective parameters from Reflection and Transmission coefficients. In contrast, methods based on local field summation allow an easy determination of the local effective properties within a gradient material.

#77425 - $15.00 USD Received 27 November 2006; revised 19 January 2007; accepted 19 January 2007

In this paper, we show that the Field Summation Method, [19, 23] used to determine the effective parameters of a metamaterial also provides visual clues of what a negative permeability stands for in a complex material. In a first part, we introduce the different Field Summation approaches that have been proposed in the literature. We indicate our calculation procedure using the HFSS commercial software. Then we compute the permeability of a metamaterial using this approach, and check that the results are consistent with other approaches. We provide videos of the time-dependent magnetic field within the unit cell of a metamaterial at several frequencies. In this way, we are able to show the configuration of the fields relevant in the evaluation of the permeability for both positive and negative permeabilities, and also purely imaginary permeability. We provide a direct and visual clue of the "negative permeability" behaviour.

In a third part, we use the same Field Summation Method to compute the permeability of thicker slabs of metamaterials. We provide pictures of the amplitude of the magnetic field in the relevant regions of the material for frequencies near the resonance. This further supports the relevance of the field summation method both as a calculation method, and a visual help for result interpretation.

The validity of the method is discussed, and further opportunities are presented.

2. Field summation methods

Let us consider a slab of material consisting of one cell that is reproduced a finite number of times along the thickness dimension *y*, and has an infinite periodic extension in the (*x*, *z*) plane. As a convention, the incoming wave has a ***k*** vector along *y*, and it is polarized with ***E*** along *z* and ***H*** along *x*. Notations are indicated on Fig. 1, where the extension in the (*x*, *z*) plane has been limited to one cell.

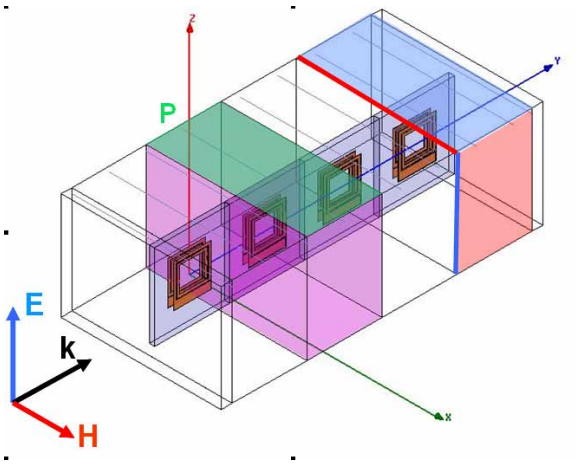

Fig. 1. Slab of periodic medium illuminated by an incoming wave: notations, and averaging zones used in different Field Summation Methods.

Rytov derived the expressions of the electromagnetic fields in a finely stratified two-component media [24]. To our knowledge he was the first to propose the determination of ε and μ for a composite by a Field Summation method. He defined the effective permeability as the volume average of the induction ***B***, over the volume average of the ***H*** field, and proposed a similar expression for the permittivity:

$$\mu_0.\mu_{V/V} = \frac{\langle B_x \rangle_{xyz}}{\langle H_x \rangle_{xyz}} \qquad \varepsilon_0.\varepsilon_{V/V} = \frac{\langle D_z \rangle_{xyz}}{\langle E_z \rangle_{xyz}} \tag{1}$$

#77425 - $15.00 USD Received 27 November 2006; revised 19 January 2007; accepted 19 January 2007

where $\langle\ \rangle_{xyz}$ is the volume average on a unit cell. The corresponding volume is represented in pink on Fig. 1.

This Field Summation approach will therefore be designated as a Volume/Volume average. Using the expression of the fields he had derived in a lamellar media, Rytov was able to propose analytic expressions of $\varepsilon_{V/V}$ and $\mu_{V/V}$ for such a media. However, it soon become clear that in the case where highly conductive materials were involved, the quantities ε and μ defined as the Volume/Volume averages could not be used to derive Fresnel Reflection and Transmission coefficients. For a composite made of non magnetic materials, $\boldsymbol{B}=\mu_0.\boldsymbol{H}$ everywhere. As a consequence, the permeability $\mu_{V/V}$ of any composite made of non magnetic materials is unity. This contradicts many experiments showing that significant permeability levels can be measured on composites based on inclusions with metallic non magnetic patterns.

From this widely shared statement, three approaches were conducted in order to obtain an adequate Field Summation method. A Russian team suggested to perform the volume average over the irrotational fields $\boldsymbol{E}$ and $\boldsymbol{H}$, that is the fields in the absence of currents [25]. However, this approach may not be well suited for easy implementation in electromagnetic simulation software. J. B. Pendry suggested taking the ratio of a surface integral over a line integral. This approach was recently refined and results obtained using the HFSS commercial software [18] have been provided. In this Surface/Line averaging method, the constitutive parameters are expressed as:

$$\mu_0.\mu_{S/L} = \frac{\langle B_x \rangle_{yz}}{\langle H_x \rangle_x}.\frac{n_y kd}{\sin(n_y kd)}$$

$$\varepsilon_0.\varepsilon_{S/L} = \frac{\langle D_z \rangle_{xy}}{\langle E_z \rangle_z}.\frac{n_y kd}{\sin(n_y kd)} \qquad (2)$$

$\langle\ \rangle_{yz}$ corresponds to the averaging over one face of the unit cell in the (y, z) plane, shown in pale red on Fig. 1, and $\langle\ \rangle_x$ corresponds to the averaging over one edge of the cell, shown in red on Fig. 1. The appropriate averaging zones to obtain ε are represented in blue. In this approach, the refractive index n_y has to be extracted from the electromagnetic simulation software, in addition to the field averages. The validity of these two approaches is backed by physical arguments, but no direct proof has been given that the definitions of the effective quantities are adequate to perform calculation of the reflection and transmission coefficients.

A third approach was proposed in 2000 in order to find an appropriate definition of the effective parameters though a retrieval procedure [23]. This approach established that the following quantities:

$$\mu_0.\mu_{V/S} = \frac{\langle B_x \rangle_{xyz}}{\langle H_x \rangle_{xy}} \qquad \varepsilon_0.\varepsilon_{S/V} = \frac{\langle D_z \rangle_{xy}}{\langle E_z \rangle_{xyz}} \qquad (3)$$

yield the proper Fresnel coefficients. $\langle\ \rangle_{xy}$ corresponds to the averaging over one face of the cell labelled P and pictured in light green on Fig. 1. This method may be designated as Volume/Surface averaging method. These expressions were obtained within a certain range of assumption, and in particular the P face should be normal to the electric field, and no conducting element should cross this plane. This approach has been applied successfully to determine the analytic expressions for ε and μ of lamellar composites [23], for the

#77425 - $15.00 USD Received 27 November 2006; revised 19 January 2007; accepted 19 January 2007

permeability of materials made of hollow conductors [26], and for the permittivity of wire medium [27]. More recently, this approach has been implemented numerically and applied to metamaterials [19].

3. Numerical details

Metamaterial made of compact inductive patterns are considered. The inductive pattern consists of a pair of planar 2-turns coils, already described in Ref. [19] and sketched on Fig. 1. The HFSS commercial software has been used to compute the field inside slabs of metamaterials, along with reflection and transmission coefficients for a normal incidence. In order to simulate an infinite lattice along the *x* and *z* directions we defined boundary conditions at the lateral ends of the unit cell. Perfect magnetic walls are assigned to faces perpendicular to the incident magnetic field, and perfect electric walls are assigned to faces perpendicular to the incident electric field. The thickness along the *z* direction is finite, corresponding to either one or four metamaterial patterns. Spacers with 2mm thickness and the electromagnetic properties of void are inserted on each side of the slab, to account for the finite dimensions of the structure.

The HFSS Software includes a field calculator which is convenient to perform field summation on user-defined regions of the cell. The appropriate regions are the planar facet P and the volume V. The real and imaginary parts of each component of the field averages provided by the software are then used to compute the complex quantities $\varepsilon_{S/V}$ and $\mu_{V/S}$ according to Eq. (3). It can be noted that since no magnetic materials are used, $\boldsymbol{B}=\mu_0.\boldsymbol{H}$ everywhere, and the permeability deduced form Eq. (3) writes:

$$\mu_{V/S} = \frac{\langle H_x \rangle_{xyz}}{\langle H_x \rangle_{xy}} \tag{4}$$

The fields can be visualized on the different selected regions and time animations can be produced. In order to produce an intuitive view of the fields that contributes to the volume integral $\langle H_x \rangle_{xyz}$, we also defined as an object the plane M that is parallel to the P plane, and that includes the axis of the inductive pattern. The representation of the fields in this M "middle plane" provides a good view of what is happening in the volume of the inductive structure.

4. Results

4.1. Thin slabs

Calculations were first performed on a slab of metamaterial containing only one pattern in its thickness. The permeability and permittivity extracted using Volume/Surface Field Summation are represented on Fig. 2(a). These values were used to compute the Reflection and Transmission coefficients of the slab using the Fresnel equations. Figure 2(b) shows the comparison between the values predicted from this Field Summation approach, with the raw values for R and T obtained directly from the HFSS Software. Excellent agreement is observed. This supports the validity and the efficiency of our Field Summation method.

#77425 - $15.00 USD Received 27 November 2006; revised 19 January 2007; accepted 19 January 2007

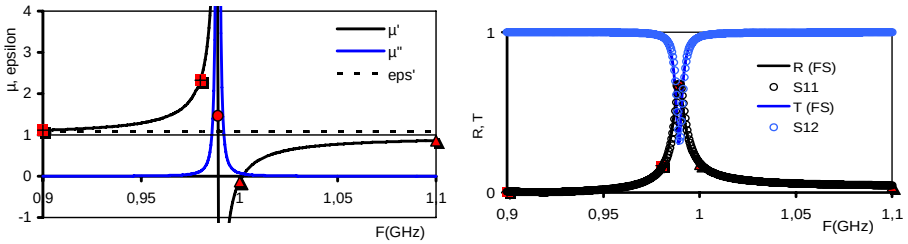

(a) (b)

Fig. 2. (a). Permeability and permittivity obtained by field averaging on a single scatterer thick metamaterial slab; (b). Reflection and Transmission coefficients for the metamaterial slab, calculated using the effective parameters obtained by Field Summation (full curve); and computed in the numerical experiment (S11, S12). Red markers correspond to frequencies of Figs. 3-6.

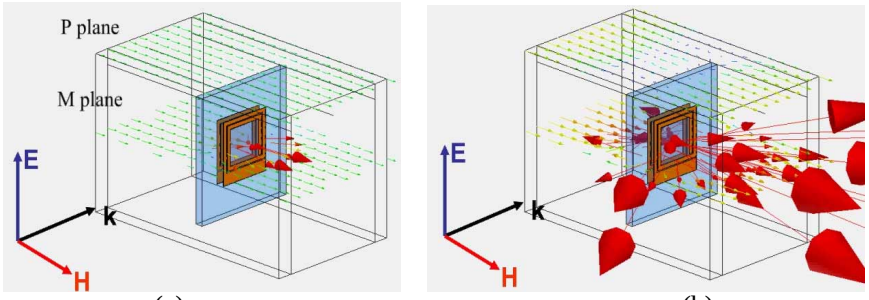

(a) (b)

Fig. 3. ***H*** field as a function of time on the P and M planes in a metamaterial: (a). (0.81 MB movie) at 0.9 GHz, the permeability is slightly larger than unity; (b). (1.56 MB movie) at 0.98 GHz, the permeability is large and positive.

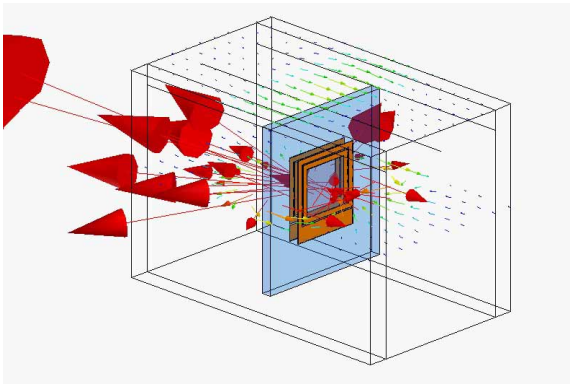

Fig. 4. (2.31 MB movie) ***H*** field as a function of time on the P and M planes in a metamaterial at the resonance frequency F=0.99 GHz

#77425 - $15.00 USD Received 27 November 2006; revised 19 January 2007; accepted 19 January 2007

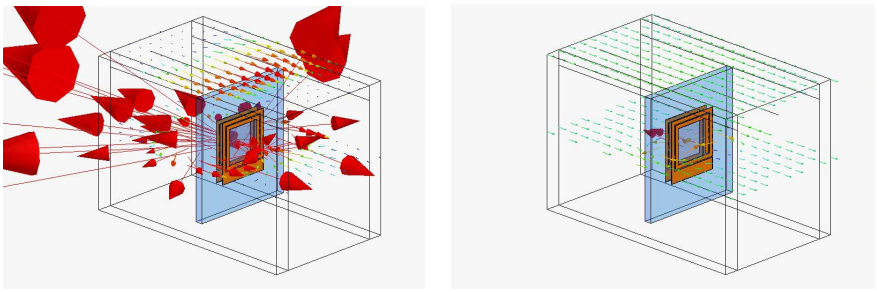

Fig. 5. ***H*** field as a function of time on the P and M planes in a metamaterial: (a) (1.89 MB movie) at 1 GHz, the permeability is negative; (b) (0.75 MB movie) at 1.1 GHz, the permeability is slightly lower than unity.

In order to gain an improved intuitive understanding, we saved animations of the magnetic field as a function of time for different frequencies. The length of the vectors corresponds to the logarithm of their magnitude. Figure 3(a) represents the field at F=0.9 GHz. At this frequency, the permeability is slightly larger than unity. While the magnitude and orientation of the ***H*** vector in the P plane is hardly affected by the resonator, it is clear from the animation that the field in the zone inside the resonator is larger than the exciting field, and oriented in the same direction. This contribution leads to $\langle H_x \rangle_{xyz} > \langle H_x \rangle_{xy}$, and therefore $\mu>1$. Figure 3(b) provides an animation of the ***H*** field at a frequency closer to the resonance, but still below the resonance, corresponding to a large positive permeability according to Fig. 2(a). The field on the upper P plane is significantly affected by the resonator underneath, but the overall direction of the average of ***H*** over P can still be estimated at first sight. In view of Eq. (4), it is clear from the animation that the very large ***H*** field inside the resonator, in phase with the average field in the P plane, accounts for the large positive permeability at this frequency.

Figure 4 provides an animation at the resonance frequency, where the permeability is imaginary and large. The direction of the ***H*** field averaged over the P plane is not easily deduced from visual observation, since opposite directions are present in the plane. One would expect a $\pi/2$ phase difference between $\langle H_x \rangle_{xy}$ and $\langle H_x \rangle_{xyz}$, which is not obvious. However, in view of Eq. (4), it is clear that the modulus of the permeability is very large at this frequency, since the ***H*** field in the M plane is very large compared the field in the P plane.

At frequencies just above the resonance, the permeability is negative [Fig. 5(a)], and at higher frequencies, the permeability is positive but still smaller than unity. The fields associated to a permeability smaller than unity are depicted on the animations of Fig. 5. It is evident that the field in the P plane has a direction opposite to the field inside the resonator. Because of this diamagnetic behaviour in the volume of the cell, the volume average in Eq. (4) is smaller than the surface average in the P plane. As a consequence the permeability is lower than unity. In the case the magnitude of the field is very large in the resonator as in Fig. 5(a), this contribution is dominant in the volume average $\langle H \rangle_{xyz}$, and as a consequence the permeability is negative. So this provides a very simple clue of what is happening inside the metamaterial that has a negative permeability.

4.2. Thick slab of metamaterial with damped behaviour

Other investigations were performed on a 4-resonators thick slab of metamaterial. The resonator is still a compact spiral pattern, but it is made of a resistive metal ($\sigma=5\times10^5$S/m). The permeability and permittivity obtained using our Field Summation method are pictured on Fig. 6(a). The Field Summation procedure is performed for each of the 4 cells, and it yields comparable results. It can be seen that the permeability has a damped behaviour, with low maximum, but large bandwidth. The Reflection and Transmission coefficients calculated from

#77425 - $15.00 USD Received 27 November 2006; revised 19 January 2007; accepted 19 January 2007

the Fresnel equations using the averaged values of Fig. 6(a) are compared on Fig. 6(b) to the coefficients obtained directly from the software. A fair agreement is obtained. This further established the validity of the method.

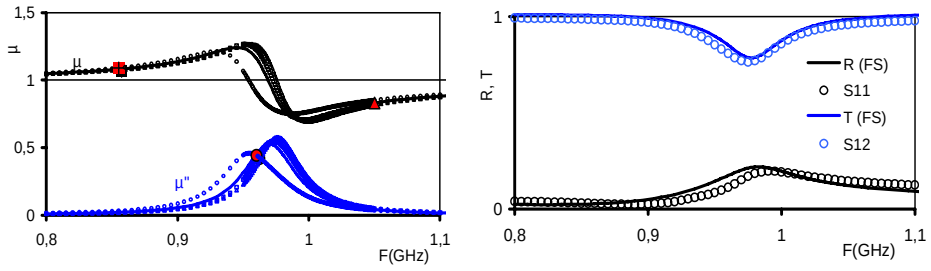

(a) (b)

Fig. 6. (a). Permeability of a 4-scatterer thick metamaterial made with a resistive metal, computed using the Field Summation method; red markers correspond to frequencies illustrated on Fig. 7; (b). Reflection and Transmission coefficients computed from the effective parameters obtained by the field averaging method, and comparison with S11 and S12 values obtained directly from the simulation software.

Figure 7 provides animations of the ***H*** field both in the P and M plane below the resonance (a), at the resonance (b), and above the resonance (c). Though the thickness of the material is somewhat smaller than a quarter wave, propagation can be clearly seen on the animations. The field maps easily reveal whether $\mu>1$ or $\mu<1$. In addition, Fig. 7(b) provides a convincing view of a $\pi/2$ phase difference between the field in the P plane and inside the resonator, responsible for the imaginary permeability at the resonance.

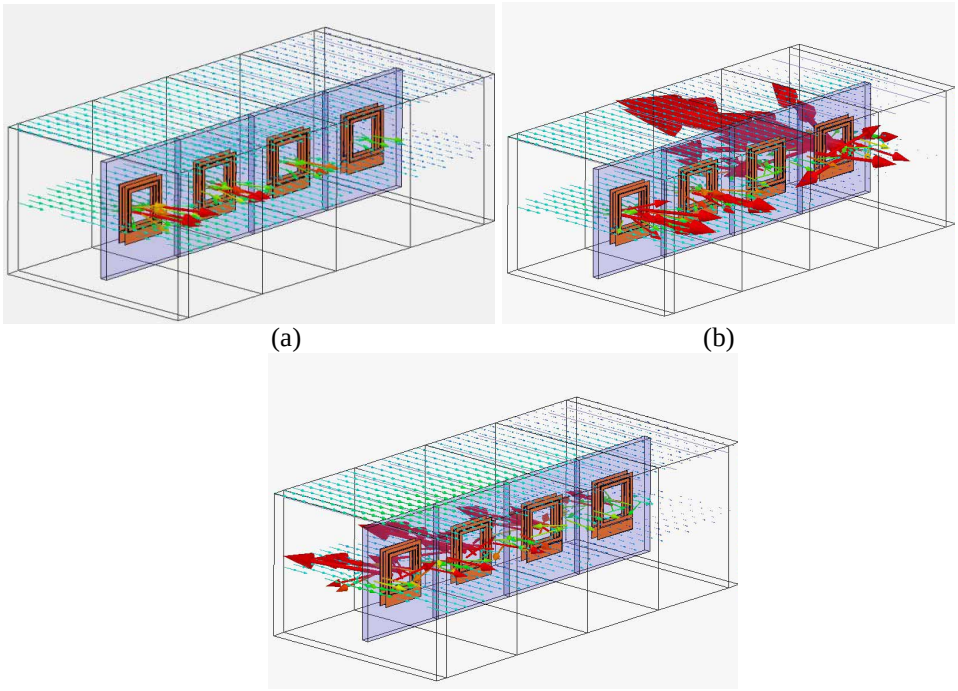

(a) (b)

(c)

Fig. 7. ***H*** field in a 4-scaterrer thick metamaterial slab made with a resistive metal; (a) (2.10 MB movie) at 0.85 GHz ($\mu>1$); (b) (2.48 MB movie) at 0.96 GHz (μ is imaginary); (c) (2.38 MB movie) at 1.05 GHz ($\mu<1$).

#77425 - $15.00 USD Received 27 November 2006; revised 19 January 2007; accepted 19 January 2007

4.3. Thick slabs of metamaterial with highly resonant behaviour

A similar 4-scatterers thick metamaterial made of copper ($\sigma=6\times10^7$S/m) was also investigated numerically. The reflection and transmission coefficients are pictured on Fig. 8. The Field Summation procedure was performed for each of the 4 cells, yielding very dissimilar results. As investigated previously [19], this is an indication that the metamaterial can not be adequately described by effective parameters that should be independent on the material thickness. So this is not a failure of the Field Summation method, but rather a limitation of any homogenization procedure.

Because of the complexity of the field maps, it was found that animations representing the fields in the P and M plane were confusing. For that reason, Fig. 9 gives a snapshot of the ***H*** field in the P plane and in the M plane at a given time, for a frequency F=1.04 GHz. It can be seen that strong inhomogeneities are present in the P plane, that can not be attributed to some propagation effects. For a thick slab of material for the two left cells, is expected to be oriented in the same direction. Figure 9(b) shows that $\langle H \rangle_M$ has different orientation for adjacent cells, in contrast with observations on Figs. 7(a) and 7(c), where the material can be properly described through effective parameters. The ***H*** field lines draw closed contours that encompass two scatterers. This is an evidence of strong interactions between neighbouring scatterers that prevent a valid homogenization procedure.

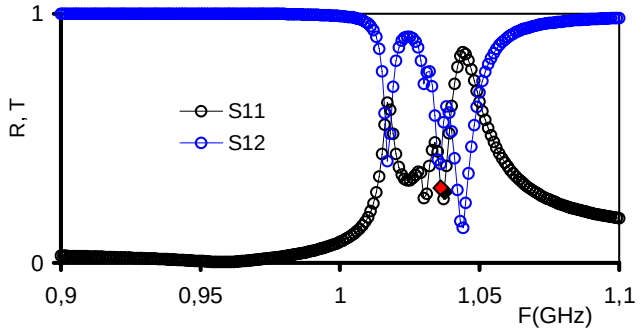

Fig. 8. Reflection and Transmission coefficients for a 4-scatterrer thick slab consisting of highly resonant patterns, computed using the simulation software.

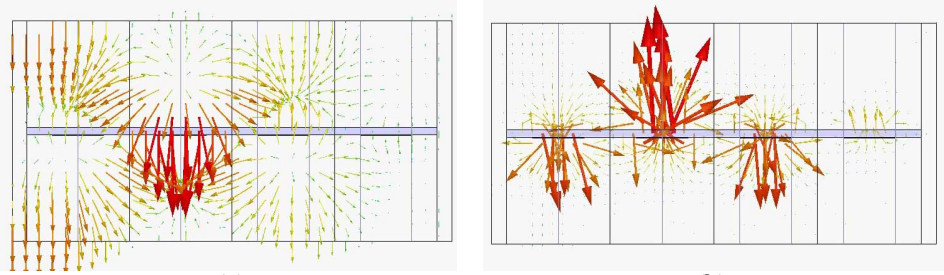

Fig. 9. ***H*** field in a 4-scatterrer thick slab consisting of highly resonant patterns, at a frequency 1.04 GHz; (a) Top view of the P plane; (b) Top view of the M plane.

5. Discussion

It is clear on Figs. 2(b) and 6(b) that the Volume/Surface Field Summation method provides values of ε and μ that lead to the correct reflection and transmission coefficients. In addition,

#77425 - $15.00 USD Received 27 November 2006; revised 19 January 2007; accepted 19 January 2007

it also provides direct insights on cases where homogenisation may not be adequate in a given frequency range. The representation of the fields associated to non-unit permeability may be valuable to share an intuitive representation, in particular within the optics community. In addition, Field Summation methods can be used to investigate inhomogeneous [28] or gradient-based metamaterials [20], which are showing extremely promising features [21].

It is tempting to use this method to investigate negative index materials. However, a number of such composites have infinite wires along the E field direction, while our demonstration of the field summation method relied on the absence of conductor crossing the P plane [23]. This restriction appears to be shared by the Surface/Line method also [18]. As previously suggested, a way to go around this difficulty may be to replace the infinite wire by finite pieces of wires separated by small planar capacitive elements parallel to P, the P face of the cell being between the plates or against one of the capacitive plate. But it is also possible that in many cases of interest, the Volume/Surface method can be applied directly to composites with infinite wires in the E field direction. This has been done successfully in Ref. [27] for negative permittivity wire media made of magnetic wires.

One may wonder whether the Volume/Surface Field Summation method presented here, and the Surface/Line method by Smith and Pendry, are equivalent or not. Though the averaging zones illustrated on Fig. 1 are very dissimilar, they may give identical predictions in some or all cases. As an example of different methods yielding similar results, it has been shown that the Volume/Surface method was equivalent to the Volume/Volume method for the determination of the permittivity of a wire media [27, 29]. A more exhaustive comparison would be very valuable, either to establish equivalence between the different approaches, with possible restrictions, or to provide examples where the different approaches yield different predictions.

It is now well known that the description of metamaterials as homogeneous effective media is in some cases inadequate or limited in validity, independently of a particular homogenization procedure [16, 30, 31]. A clear advantage of the Volume/Surface method is that its derivation has put forward several conditions that that are required to perform homogenization [23]. In particular, only one mode should propagate in the material, away from the interface. This condition is not met in the cased of Figs. 8 and 9.

A present advantage of the Volume/Surface method in its validity region is the direct connection established in Ref. [23] between the retrieved parameters and their ability to account for both the reflection and transmission coefficients at an interface, and the index. As a consequence, it is straightforward to establish that the reflection and transmission on any slab of finite thickness can be obtained. In contrast, a retrieval procedure from the complex reflection and transmission coefficients, though it yields the appropriate number of equations to determine ε and μ, may sometime lead to multiple solutions.

The numerical implementations of the Volume/Surface and the Surface/Line approaches have been performed using different options of the HFSS software. In Ref. [18], the eigensolver module was used, that provides the fields within the infinite medium. It also provides directly the index, which is useful in Eq. (2). However, as stated in Ref. [18], it may not be used in frequency regions where losses are high. This is of course damageable to determine resonance frequencies of the effective parameters, and full spectral features. In our case, we used another module of HFSS that provides the fields on a finite slab of material. However, it is believed that both field summation methods can be adapted on both HFSS options.

6. Conclusion

Several groups have proposed to determine the effective parameters of a composite as the ratio of appropriate local field averages. Similarities and differences between these approaches have been indicated and discussed in this paper. The “Volume/Surface” method is illustrated here. This method had emerged through the search of an adequate definition of the effective parameters consistent with Reflection and Transmission experiments. This method has been implemented numerically using the commercial HFSS software and applied to

#77425 - $15.00 USD Received 27 November 2006; revised 19 January 2007; accepted 19 January 2007

metamaterials. The effective parameters obtained using this method are found to be relevant. In addition, this it is shown that appropriate field maps produced by the software can be easily interpreted in terms of sign and magnitude of the permeability. This works opens several opportunities, such as the application of the method to other types of metamaterials, including gradient media and wire-based negative index media. Other opportunities include the comparison between the different field summation approaches, and their implementation in the most popular electromagnetic software.

#77425 - $15.00 USD Received 27 November 2006; revised 19 January 2007; accepted 19 January 2007